Inorg. Chem. **1986**, *25*, 4245–4248

Contribution from the Research School of Chemistry, Australian National University, Canberra, ACT 2601, Australia, and Institut für anorganische Chemie, Johannes Gutenberg Universität, D-6500 Mainz, FRG

High-Spin → Low-Spin Relaxation Kinetics and Cooperative Effects in the [Fe(ptz)$_6$](BF$_4$)$_2$ and [Zn$_{1-x}$Fe$_x$(ptz)$_6$](BF$_4$)$_2$ (ptz = 1-Propyltetrazole) Spin-Crossover Systems

Andreas Hauser,*[†] Philipp Gütlich,[‡] and Hartmut Spiering[‡]

Received April 3, 1986

[Fe(ptz)$_6$](BF$_4$)$_2$ (ptz = 1-propyltetrazole) and the mixed crystals [Zn$_{1-x}$Fe$_x$(ptz)$_6$](BF$_4$)$_2$ are Fe(II) spin-crossover compounds that exhibit light-induced excited-spin-state trapping. It is shown that (a) for $x \leq 0.1$ a single-ion treatment of both the spin equilibrium (ΔH_{HL} = 510 (12) cm^{-1}, ΔS_{HL} = 5.1 (2) cm^{-1}/K at T = 100 K) and the relaxation from the excited high-spin state ($E_a°$ = 810 (30) cm^{-1}, $A \sim 10^5$/s) is appropriate and (b) for $0.2 \leq x \leq 1$ cooperative effects observed in the relaxation from the high-spin state are of long-range nature and therefore of elastic rather than of electronic origin.

1. Introduction

Spin-equilibria and spin-crossover kinetics in Fe(II) compounds exhibiting thermal low spin (LS) → high spin (HS) transitions have been the object of several studies, using mainly Mössbauer spectroscopy and magnetic susceptibility measurements for the former[1] and temperature-jump techniques,[2,3] temperature quenching,[4] and laser flash photolysis[5,6] for the latter. Most of the kinetics experiments up to date have been performed on spin-crossover systems in solution at temperatures around 293 K.

Recently Decurtins et al.[7,8] showed that in a number of Fe(II) compounds, which exhibit thermal spin transitions, light-induced LS (^{1}A$_1$) → HS (^{5}T$_2$) conversion can be observed by irradiating into the ^{1}A$_1$ → ^{1}T$_1$ ligand field absorption band (~550 nm) at temperatures well below the thermal transition temperature. A mechanism for this phenomenon, subsequently termed "light-induced excited-spin-state trapping (LIESST)", was proposed,[8] involving intersystem crossing from the excited ^{1}T$_1$ state to an intermediate low-lying ^{3}T$_1$ state and from there to the ^{5}T$_2$ state, where at sufficiently low temperatures the system remains trapped, the large difference of 0.1–0.2 Å^2 in equilibrium bond lengths of the two spin states effectively separating the potential wells (see Figure 1). The trapped HS state of course relaxes back to the LS state thermally at some higher temperature, but the system can also be pumped back to the LS state by irradiating into the ^{5}T$_2$ → ^{5}E absorption band (~850 nm).[9]

[Fe(ptz)$_6$](BF$_4$)$_2$ (ptz = 1-propyltetrazole) in the solid state shows an extremely sharp thermal spin transition with hysteresis around 130 K.[10] It exhibits the normal LIESST effect below 50 K; above that temperature it relaxes back to the ^{1}A$_1$ state with a strong deviation from first-order kinetics.[8] At 10 K the system remains trapped indefinitely (i.e., after 14 h at 10 K no relaxation could be observed), excluding any tunneling processes. Both the first-order phase-transition-like thermal spin crossover and the relaxation from the light-induced HS state indicate that cooperative (lattice) effects are important. Thermal spin crossover and LIESST are also observed in dilute [Zn$_{1-x}$Fe$_x$(ptz)$_6$](BF$_4$)$_2$ ($x \approx 0.1$).[9]

In this paper it is shown that for the dilute material ($x \leq 0.1$), where cooperative effects are expected to be small, the thermal spin equilibrium as well as the relaxation kinetics can be described in terms of the single-ion (unimolecular) model also used in solution work,[2,3] and the thermodynamic parameters of the spin equilibrium ΔH_{HL} and ΔS_{HL} and the activation parameters of the relaxation are given. These single-ion parameters are used to present a quantitative analysis of the cooperative effects influencing the thermal relaxation in the more concentrated materials ($0.2 \leq x \leq 1$), making use of the lattice expansion model developed by Spiering et al.[11]

2. Experimental Section

[Fe(ptz)$_6$](BF$_4$)$_2$ was prepared according to a procedure previously described.[10] Pure [Zn(ptz)$_6$](BF$_4$)$_2$ was prepared in the same way. Single crystals in the form of colorless hexagonal plates up to several millimeters in diameter of the pure [Fe(ptz)$_6$](BF$_4$)$_2$ salt as well as the mixed crystals [Zn$_{1-x}$Fe$_x$(ptz)$_6$](BF$_4$)$_2$ were grown from aqueous solutions. The mole fraction x of Fe(II) in the mixed crystals was determined by AAS and generally found to be lower than the mole fraction in the corresponding solution; i.e., a 1:4 [Fe(ptz)$_6$]$^{2+}$:[Zn(ptz)$_6$]$^{2+}$ mixture in solution resulted in crystals with $x \approx 0.1$. The thermal spin crossover is accompanied by a drastic change in color: below 130 K the colorless crystals turn deep purple.

Unpolarized single-crystal absorption spectra with the light propagating along the hexagonal crystal axis were recorded with a Cary 17 spectrometer. The crystals were mounted on small copper plates with machined apertures, which in turn were mounted on a copper sample holder. The samples were cooled by the helium gas flow tube technique to below 10 K. In order to quantitatively trap the Fe(II) in the HS state, the crystals were irradiated for 10 min with a 150-W xenon arc lamp, while the temperature was kept below 10 K. HS → LS relaxation curves were obtained by recording the time dependence of the optical density (OD) of the ^{1}A$_1$ → ^{1}T$_1$ transition at the OD$_{max}$ wavelength of 545 nm at constant temperatures. The temperature was controlled with a two-stage heating system: a first heater coil was placed in the cold helium stream, heating it up to ~50 K; for fine tuning a second heater coil situated on the sample holder was used. The temperature was measured with a gold–iron/chromel thermocouple in contact with the crystal mount a fraction of a millimeter away from the crystal. The reference junction was kept at liquid-nitrogen temperature. This arrangement resulted in a heatup time of less than 20 s from ~50 K (where no noticeable relaxation takes place) to the temperature at which the curve was to be recorded. Temperature stability during the recording of a curve was better than ±0.2 K; the relative accuracy between curves of one series of measurements is estimated to be within 0.5 K, and that between different series ~1.5 K.

3. Results and Discussion

3.1. The Spin-Equilibrium in [Fe(ptz)$_6$](BF$_4$)$_2$ and [Zn$_{1-x}$Fe$_x$(ptz)$_6$](BF$_4$)$_2$. In Figure 2a,b are shown the visible absorption spectra in the region of d–d transitions at various temperatures for pure [Fe(ptz)$_6$](BF$_4$)$_2$ and doped [Zn$_{1-x}$Fe$_x$(ptz)$_6$](BF$_4$)$_2$ ($x \approx 0.1$), respectively. In Figure 3 are plotted the normalized

---

[†] Australian National University.

[‡] Johannes Gutenberg Universität.

---

(1) Gütlich, P. In *Structure and Bonding*; Springer-Verlag: Berlin, 1981; Vol. 44.

(2) Beattie, J. K.; Binstead, R. A.; West, R. J. *J. Am. Chem. Soc.* **1978**, *100*, 3044.

(3) Dose, E. V.; Hoselton, M. A.; Sutin, N.; Tweedle, M. F.; Wilson, L. J. *J. Am. Chem. Soc.* **1978**, *100*, 1141.

(4) Ritter, G.; König, E.; Irler, W.; Goodwin, H. A. *Inorg. Chem.* **1978**, *17*, 224.

(5) McGarvey, J.; Lawthers, I. *J. Chem. Soc., Chem. Commun.* **1982**, 906.

(6) DiBenedetto, J.; Arkle, V.; Goodwin, H. A.; Ford, P. C. *Inorg. Chem.* **1985**, *24*, 456.

(7) Decurtins, S.; Gütlich, P.; Köhler, C. P.; Spiering, H.; Hauser, A. *Chem. Phys. Lett.* **1984**, *105*, 1.

(8) Decurtins, S.; Gütlich, P.; Hasselbach, K. M.; Hauser, A.; Spiering, H. *Inorg. Chem.* **1985**, *24*, 2174.

(9) Hauser, A. *Chem. Phys. Lett.* **1986**, *124*, 543.

(10) Franke, P. L.; Haasford, J. G.; Zurr, A. P. *Inorg. Chim. Acta* **1982**, *59*, 5.

(11) Spiering, H.; Meissner, E.; Köppen, H; Müller, E. W.; Gütlich, P. *Chem. Phys.* **1982**, *68*, 65.

0020-1669/86/1325-4245$01.50/0

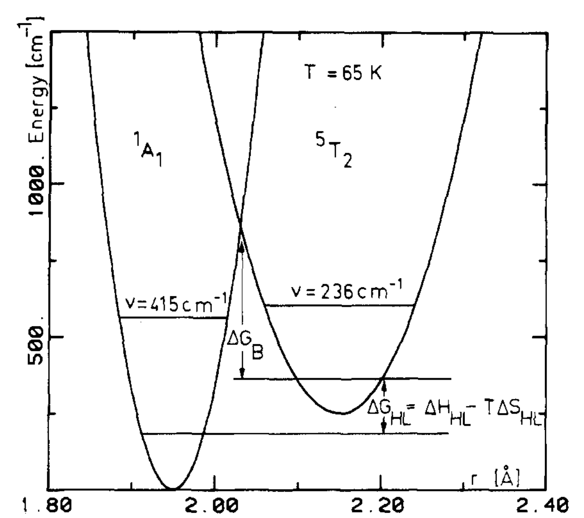

Figure 1. Semiquantitative representation of the low-spin $^1A_1$ and the high-spin $^5T_2$ thermodynamic potential wells in $[Fe(ptz)_6](BF_4)_2$ (harmonic potentials) at 65 K. The free energy difference between the HS and the LS states is $\Delta G_{HL} = 180$ cm^{-1}. The barrier $\Delta G_B \sim 530$ cm^{-1} is close to $E_a{}^\circ = 810$ cm^{-1}, the activation energy obtained from experiment.

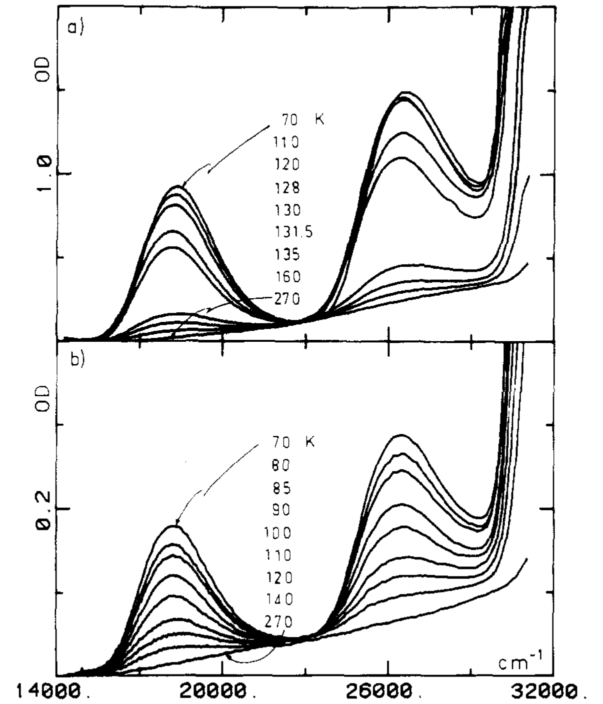

Figure 2. Single-crystal absorption spectra at various temperatures for (a) $[Fe(ptz)_6](BF_4)_2$ ($T\uparrow$) and (b) $[Zn_{1-x}Fe_x(ptz)_6](BF_4)_2$ ($x \approx 0.1$) in the region of the low-spin $^1A_1 \rightarrow {}^1T_1$ ($\nu_{max} = 18\,400$ cm^{-1}) and $^1A_1 \rightarrow {}^1T_2$ ($\nu_{max} = 26\,650$ cm^{-1}) d–d transitions.

intensities of the low-energy absorption band of the LS state, namely the $^1A_1 \rightarrow {}^1T_1$ transition. The pure material exhibits the first-order phase-transition-like behavior also observed in magnetic susceptibility measurements,[10] due to cooperative effects. In the dilute material (up to $x \approx 0.1$) such effects are expected to be small, and the observed intensity vs. temperature curve can be interpreted as a continuous LS $\rightleftarrows$ HS equilibrium with

$$\Delta G_{HL} = G_{HS} - G_{LS} = H_{HS} - H_{LS} - T(S_{HS} - S_{LS}) = \Delta H_{HL} - T\Delta S_{HL} = -k_BT \ln K_{HL} = -k_BT \ln \frac{1-\gamma_{LS}}{\gamma_{LS}} \quad (1)$$

where γ_{LS} is the low-spin fraction. Ignoring the fact that the effective transition moment of the $^1A_1 \rightarrow {}^1T_1$ transition is not quite temperature independent (vibronic intensity), the low-spin fraction

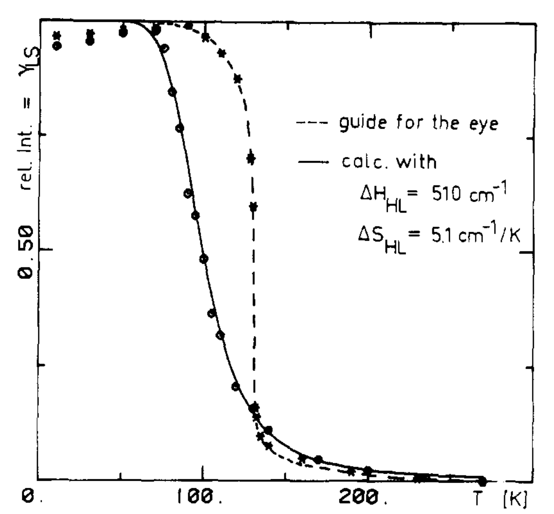

Figure 3. Relative intensity of the $^1A_1 \rightarrow {}^1T_1$ transition vs. temperature for (*) $[Fe(ptz)_6](BF_4)_2$ and (⊙) $[Zn_{1-x}Fe_x(ptz)_6](BF_4)_2$ ($x \approx 0.1$).

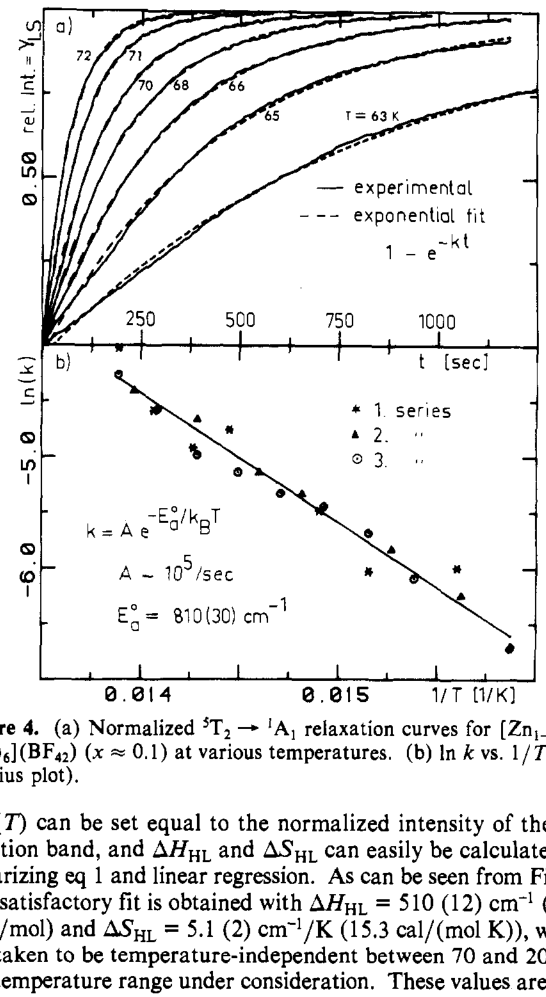

Figure 4. (a) Normalized $^5T_2 \rightarrow {}^1A_1$ relaxation curves for $[Zn_{1-x}Fe_x(ptz)_6](BF_{42})$ ($x \approx 0.1$) at various temperatures. (b) ln k vs. $1/T$ (Arrhenius plot).

$\gamma_{LS}(T)$ can be set equal to the normalized intensity of the absorption band, and ΔH_{HL} and ΔS_{HL} can easily be calculated by linearizing eq 1 and linear regression. As can be seen from Figure 3, a satisfactory fit is obtained with $\Delta H_{HL} = 510$ (12) cm^{-1} (1.46 kcal/mol) and $\Delta S_{HL} = 5.1$ (2) cm^{-1}/K (15.3 cal/(mol K)), which are taken to be temperature-independent between 70 and 200 K, the temperature range under consideration. These values are well within the comparatively small range generally observed for Fe(II) spin-crossover compounds.[2,3] This analysis is rather crude, because it assumes that there is only one energy difference ΔH_{HL} involved, completely neglecting the splitting of the $^5T_2$ state into the nine components due to an axial crystal field and spin–orbit coupling.[12]

3.2. $^5T_2 \rightarrow {}^1A_1$ Relaxation Kinetics in $[Zn_{1-x}Fe_x(ptz)_6](BF_4)_2$ ($x \approx 0.1$). Figure 4a shows the relaxation curves from the light-induced trapped $^5T_2$ state back to the $^1A_1$ state for the dilute $[Zn_{1-x}Fe_x(ptz)_6](BF_4)_2$ ($x \approx 0.1$) at various temperatures. Exponential fits to these curves, according to

---

[12] Griffith, J. S. In *The Theory of Transition Metal Ions*; Cambridge University Press: Cambridge, U.K., 1961; p 357.

$$\gamma_{LS}(t) = 1 - e^{-kt} \qquad (2)$$

were performed and are quite satisfactory. This indicates once more that for $x \leq 0.1$ cooperative effects are small. In Figure 4b are shown the Arrhenius plot for the resulting rate constants and the fit according to the Arrhenius equation

$$k = Ae^{-E_a°/k_BT} \qquad (3)$$

where $E_a°$ is the activation energy for $x \leq 0.1$. An activation energy $E_a°$ of 810 (30) cm^{-1} and a frequency factor $A \approx 10^5/s$ result. According to absolute rate theory[2,13] k for the back-relaxation from the HS state to the LS state is given by

$$k = \frac{k_BT}{h}\kappa e^{\Delta S_{LH}^*/k_B}e^{-\Delta H_{LH}^*/k_BT} \qquad (4)$$

where $\Delta H_{LH}^* = H_{LS}^* - H_{HS}$, $\Delta S_{LH}^* = S_{LS}^* - S_{HS}$, and κ is the transmission coefficient, reflecting the probability of intersystem crossing. The frequency factor A of the empirical Arrhenius equation is not temperature-independent, but as rate constants are usually studied over a narrow temperature range, the Arrhenius plot gives a satisfactory fit. The relationship between the parameters obtained from an Arrhenius plot and those from an Eyring plot according to eq 4 is

$$A \approx e\frac{k_BT}{h}\kappa e^{\Delta S_{LH}^*/k_B} \qquad E_a° \approx \Delta H_{LH}^* + k_BT \qquad (5)$$

In our case the enthalpy of activation $\Delta H_{LH}^* = 760$ (35) cm^{-1} (2.18 kcal/mol) and $\kappa \exp(\Delta S_{LH}^*/k_B) \sim 3 \times 10^{-8}$. The transmission coefficient κ and ΔS_{LH}^* cannot be separated without additional assumptions. Beattie et al.[2] took a value of -1.1 cm^{-1}/K for ΔS_{LH}^*, assuming that the quintet state differs from the transition state (LS) only by its spin degeneracy.

An order of magnitude estimate of the rate constant at room temperature using eq 4 and assuming the temperature dependence of ΔH_{LH}^* and ΔS_{LH}^* to be small gives $k_{RT} \sim 10^3$–10^4/s. This is 3–4 orders of magnitude slower than generally observed in solution for Fe(II) spin-crossover compounds.[2,3]

Now we are in a position to construct the semiquantitative picture for the two states shown in Figure 1: We have ΔH_{HL} and ΔS_{HL} from section 3.1 and ΔH_{LH}^* and ΔS_{LH}^* from the above treatment. The equilibrium metal to ligand bond length in the HS state is $r = 2.15$ Å,[14] and the difference between the HS and the LS states is $\Delta r \sim 0.2$ Å. The metal–ligand stretching vibrations are 236 and 415 cm^{-1} for the HS and the LS states, respectively,[14] and we assume a metal–ligand force constant in the HS state of ~1.7 mdyn/Å. This is slightly larger than in the high-spin Fe(II) hexaaqua complex[15] with a somewhat smaller ligand field strength. Considering the assumptions made, the internal consistency is satisfactory.

3.3. $^5T_2 \rightarrow {}^1A_1$ Relaxation in $[Zn_{1-x}Fe_x(ptz)_6](BF_4)_2$ ($0.1 \leq x \leq 1$). In Figure 5a the $^5T_2 \rightarrow {}^1A_1$ relaxation curves obtained for the pure $[Fe(ptz)_6](BF_4)_2$ at various temperatures and in Figure 6a the analogous curves at a given temperature of ~65 K for various Fe(II) concentrations x are shown. The strong deviation from first-order kinetics in the case of $[Fe(ptz)_6](BF_4)_2$ is obvious, and Figure 6a demonstrates how the effect diminishes as the Fe(II) concentration is lowered. Qualitatively the cooperative effects favor the LS state because (a) the LS state is stable to higher temperatures (see Figure 2) and (b) the relaxation is faster in the pure $[Fe(ptz)_6](BF_4)_2$. The question as to the nature of the cooperative effects now arises. Both light-induced as well as thermal spin crossover are accompanied by macroscopic volume changes and sometimes, though not in our compound, by changes of the crystal structure, in which case crystals often shatter.[8] In view of this macroscopic manifestation of the large difference in metal to ligand bond length of up to 0.2 Å between HS and LS states, elastic (lattice) interactions are expected to be important, and since the ptz ligands as well as the BF_4^- counterions are fairly bulky, the Fe(II) centers are well separated and electronic interactions should be small. This means that in principle even in the pure $[Fe(ptz)_6](BF_4)_2$ the relaxation is still a single-center process, but it is strongly influenced by the surrounding medium. The "lattice expansion model" of Spiering et al.[11] provides a way

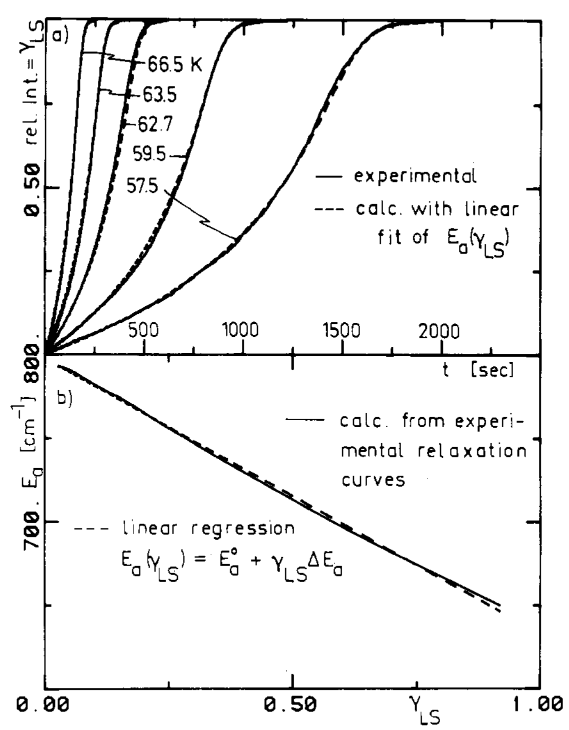

Figure 5. (a) Normalized $^5T_2 \rightarrow {}^1A_1$ relaxation curves for pure $[Fe(ptz)_6](BF_4)_2$ at various temperatures. (b) The activation energy E_a as a function of γ_{LS}. The solid line was obtained from a simultaneous fit of the five experimental curves of Figure 5a, as described in the text. The broken line is the result of a linear regression (slope $\Delta E_a = -164$ cm^{-1}; intercept $E_a° = 797$ cm^{-1}).

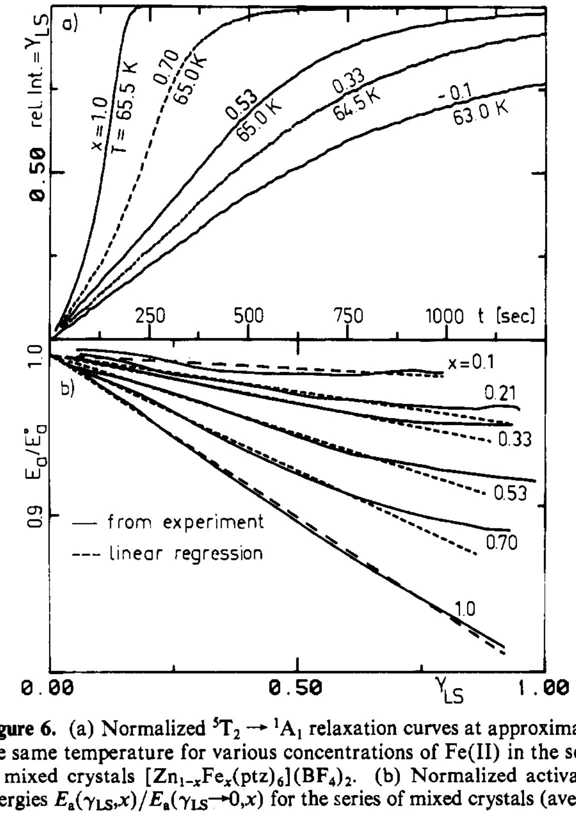

Figure 6. (a) Normalized $^5T_2 \rightarrow {}^1A_1$ relaxation curves at approximately the same temperature for various concentrations of Fe(II) in the series of mixed crystals $[Zn_{1-x}Fe_x(ptz)_6](BF_4)_2$. (b) Normalized activation energies $E_a(\gamma_{LS},x)/E_a(\gamma_{LS}\rightarrow 0,x)$ for the series of mixed crystals (average of at least five relaxation curves recorded at different temperatures for each concentration).

---

(13) Laidler, K. J. In *Chemical Kinetics*; McGraw-Hill: New York, 1965; p 88.

(14) Franke, P. L. Ph.D. Thesis, Leiden, 1982.

(15) Hupp, J. T.; Weaver, M. J. *J. Phys. Chem.* **1985**, *89*, 2795.

of analyzing our data quantitatively. The idea behind the model, which basically treats the crystal lattice as a continuum, is the following: Associated with a change in spin state is a change in volume of $V_{HS} - V_{LS}$. This volume change exerts an internal pressure, which in elastic theory is called image pressure[16] and which is proportional to the difference in volume. Summing over all the Fe(II) centers in the LS state and taking into account that in the mixed crystals there is already an internal pressure present at $\gamma_{LS} = 0$ due to the difference between V_{HS} and V_{Zn}, the total internal pressure change can be expressed by[11]

$$\Delta p \sim (V_{HS} - V_{LS})\gamma_{LS}x + (V_{HS} - V_{Zn})(1 - x) \qquad (6)$$

where x is the mole fraction of Fe(II). The second term is expected to be small because the ionic radii of Fe^{2+}(HS) and Zn^{2+} are almost the same. In the similar system of $[Fe(2\text{-pic})_3]Cl_2\cdot EtOH$ and the corresponding Zn compound $V_{Zn} - V_{HS} = 3$ Å^3,[17] whereas $V_{HS} - V_{LS} = 61$ Å^3.[18] This internal pressure acts upon each HS ion in the crystal in such a way as to increase the relaxation rate. It is not likely that the probability of the intersystem crossing from the HS to the LS potential surface and therefore the frequency factor A are influenced to any large extent by such a pressure. It is rather the activation energy E_a that is a function of Δp and therefore of γ_{LS} and x:

$$k = k(\gamma_{LS},x) = Ae^{-E_a(\gamma_{LS},x)/k_BT} \qquad (7a)$$

or

$$E_a(\gamma_{LS},x) = (\ln A - \ln k(\gamma_{LS},x))k_BT \qquad (7b)$$

The following differential equation still holds:

$$d\gamma_{LS}/dt = (k(\gamma_{LS},x))(1 - \gamma_{LS}) \qquad (8)$$

But now k is a function of $\gamma_{LS}(t)$ and x and eq 8 has no general analytical solution (eq 1 in ref 8 is not a solution, but fortunately the qualitative statements made therein remain valid). However, $E_a(\gamma_{LS},x)$ can easily be calculated by numerically differentiating the experimental $\gamma_{LS}(t)$ curves, dividing by $(1 - \gamma_{LS}(t))$, and using eq 7b with $A = 10^5$/s. In Figure 5b are shown the results of such a calculation, simultaneously fitting all five curves of Figure 5a: $E_a(\gamma_{LS},x=1)$ is, within experimental accuracy, independent of temperature in this temperature range and $E_a(\gamma_{LS}\rightarrow 0,x=1)$ is well within one standard deviation of $E_a°$, the activation energy for $x \approx 0.1$. In Figure 6b is shown $E_a(\gamma_{LS},x)/E_a(\gamma_{LS}\rightarrow 0,x)$ for the whole series of mixed crystals. The $E_a(\gamma_{LS}\rightarrow 0,x)$ values are all within one standard deviation of $E_a°$. Most strikingly, $E_a(\gamma_{LS},x)$ for the pure compound is linear in γ_{LS} over the full range of γ_{LS} and for the mixed crystals at least up to $\gamma_{LS} \sim 0.8$, suggesting that we write

$$E_a(\gamma_{LS},x) = E_a° + \gamma_{LS}(\Delta E_a(x)) \qquad (9)$$

A linear regression of $E_a(\gamma_{LS},x)$ for $\gamma_{LS} < 0.8$ for each value of x was performed, the slope giving $\Delta E_a(x)$ and all the intercepts being close to $E_a°$ for $x \approx 0.1$. If our idea of the cooperative effects is correct, namely that they are of elastic and therefore long-range origin, $\Delta E_a(x)$ should be linear in x, and Figure 7 shows this to be the case.

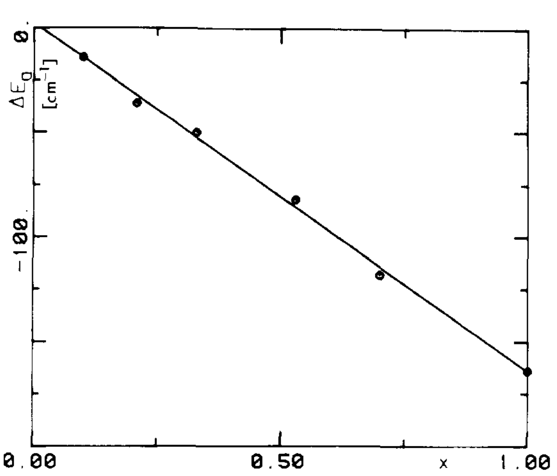

Figure 7. $\Delta E_a(x)$ as a function of the Fe(II) mole fraction x in the mixed-crystal series $[Zn_{1-x}Fe_x(ptz)_6](BF_4)_2$.

From the linear fit of $E_a(\gamma_{LS},x)$ we can now retrace our calculation back to the actual relaxation curves. Inserting eq 9 into eq 7, we can calculate $k(\gamma_{LS},x)$, which in turn can be used in a numerical integration of eq 8, resulting in calculated $\gamma_{LS}(t)$ curves. In Figure 5a are shown relaxation curves for the pure $[Fe(ptz)_6](BF_4)_2$ calculated by using $E_a° = 797$ cm^{-1} and $\Delta E_a(x=1) = -164$ cm^{-1}.

4. Conclusions

It has been shown that for $x < 0.1$ the single-ion treatment of both the spin equilibrium and the relaxation from the trapped HS state gives satisfactory results. It must be noted that $x \approx 0.1$ is already a rather high concentration as a $\Delta E_a(x\approx 0.1)$ of 15 cm^{-1} is to be expected. However, $x \approx 0.1$ is a suitable compromise for the low-concentration measurements, so that the signal is still detectable with reasonable accuracy.

Cooperative effects in the relaxation process are long range in nature, as borne out by the proportionality with the Fe(II) concentration. There is no evidence for any short-range electronic interactions of importance in this context. It is not conclusive from this work whether the long-range cooperative interaction in the HS–LS relaxation is identical or not with the elastic interaction responsible for the cooperative nature (first-order phase transition) of the thermally induced spin crossover.[11] However, the evaluation procedure for our data with an energy barrier linearly dependent on the LS fraction γ_{LS} and the concentration x of HS/LS ions was guided by the idea of elastic interactions. How pressure of a few kilobars ($\Delta p \sim f(\Delta V/V), f \sim 10^{10}$ N/m^2, $\Delta V/V \sim 10^{-2}$) can change the effective energy barrier by more than 10% is not clear, as displacements of the HS and LS potential wells due to such a pressure would be of the order of $\sim 10^{-3}$ Å, which would alter the barrier height in Figure 1 by less than 1%. Furthermore, the deviation from linearity of $E_a(\gamma_{LS},x)$ for $\gamma_{LS} > 0.8$ and $x \leq 0.7$ is puzzling, because for smaller pressure changes (as compared to $x = 1$) the linear term in an expansion series should be even more dominant. A study of the HS–LS relaxation under external pressure could give the answer to these problems.

Registry No. $[Fe(ptz)_6](BF_4)_2$, 82285-70-9.

---

(16) Eshelby, J. D. *Solid State Phys.* **1956**, *3*, 79.

(17) Mikami-Kido, M.; Saito, Y. *Acta Crystallogr., Sect. B: Struct. Crystallogr. Cryst. Chem.* **1982**, *B38*, 348.

(18) Meissner, E.; Köppen, H.; Spiering, H.; Gütlich, P. *Chem. Phys. Lett.* **1983**, *95*, 163.